Wave dispersion in a counterstreaming, cold, magnetized, electron-positron plasma

M. W. Verdon and D. B. Melrose
School of Physics, University of Sydney, New South Wales 2006, Australia
(Received 21 December 2007; published 15 April 2008)

The dispersion equation is analyzed for waves in a strongly magnetized, electron-positron plasma in which counterstreaming electrons are cold in their respective rest frames. For propagation parallel to the magnetic field the dispersion equation factorizes into equations for two longitudinal modes and four transverse modes. Instabilities occur in both longitudinal and transverse modes, with the most notable being at low wave numbers where a longitudinal branch has purely imaginary frequency. For oblique propagation at small angles, the modes reconnect at points where the parallel modes intersect, either deviating away from each another, or being separated by a pair of complex modes. In addition, intrinsically oblique branches of the dispersion equation appear. The results are applied to an oscillating model for a pulsar magnetosphere, in which the oscillations are purely temporal with a frequency well below relevant wave frequencies, and in which the counterstreaming becomes highly relativistic. We assume that the medium may be treated as time stationary in treating the wave dispersion and wave growth. The wave properties, including the wave frequency, vary periodically with the phase of the oscillations. The fastest growing instability is when the counterstreaming is nonrelativistic or mildly relativistic. A given wave can experience bursts of growth over many oscillations. Mode coupling associated with the cyclotron resonance may be effective in generating the observed orthogonally polarized modes at phases of the oscillation where the (relativistic) cyclotron and wave frequencies are comparable.

DOI: 10.1103/PhysRevE.77.046403 PACS number(s): 95.30.Qd, 95.30.Gv, 97.60.Gb, 52.35.Lv

I. INTRODUCTION

Two inadequately understood aspects in the physics of radio pulsars are how the observed radio emission is generated [1] and why there is a mixture of two orthogonally polarized modes (OPMs) in the escaping radiation [2,3]. Pulsar emission is extremely bright and can be explained only in terms of a plasma instability. However, possible instabilities seem too slow to allow effective wave growth. The growth is limited by the relativistic outflow of the plasma in two ways. First, the change in the plasma parameters along the flow path limits the growth time, with the limit being the more severe the narrower the bandwidth of the growing waves. Second, both the growth rate and the bandwidth of the growing waves decrease with increasing Lorentz factor of the streaming motion. Even for the broadest-band, fastest-growing instability [4], and for the lower Lorentz factors, $\gamma \approx 10-100$ now favored [5–7], it is difficult to account for effective growth. Rapid wave growth is required, but it seemingly precludes the most obvious interpretation of OPMs. Any instability favors one wave mode over others—the fastest growing mode—and after many *e*-folding growth lengths, the resulting radiation is effectively in this fastest-growing wave mode, and should be completely polarized in the sense of this mode. OPMs, which are an almost universal feature of the observed emission, imply that the escaping radiation is often a roughly equal mixture of two elliptically polarized modes, and that the rays corresponding to the two modes propagate along significantly different ray paths. For the ray paths to be significantly different, refraction must occur relatively close to the source region, where the wave frequency is comparable with some natural frequency of the plasma, all of which decrease rapidly with increasing height. The observations of OPMs raise two obvious problems. The first problem is how a roughly equal mixture of two modes is produced so routinely. The simplest interpretation of OPMs involves assuming that the radiation is generated as a roughly equal mixture of two modes, but this assumption seems to be excluded by the requirement for rapid growth. The second problem is that observational evidence from single pulses for relatively large circular polarization suggests that the two modes can be substantially elliptically polarized [8], implying that the polarization is imposed in a region where the (relativistic) cyclotron frequency is comparable with the wave frequency, but this occurs only at heights far above the source region in conventional models [9]. A possible way of overcoming these difficulties is provided by an oscillating model for pulsar electrodynamics, involving large-amplitude oscillations in the parallel electric field [10–12]. The large amplitude oscillations are the result of assuming that the electric field and current are not constant, and so inductive effects are important in the screening of the vacuum electric field [11]. The conventional assumption is that screening is electrostatic. Estimates of the oscillation frequency for standard pulsar parameters gives, in the center-of-mass frame of the plasma, a frequency of order 10^6 Hz. The plasma frequency calculated with the same parameters is of order 10^9 Hz. It is thus reasonable to make the assumption that the oscillations lead to a slowly varying medium when compared with radiation around the region of the plasma frequency, as discussed in this paper.

In such a model, the dominant effect is counterstreaming of the electrons and positrons, with Lorentz factors up to $\gamma_{\max} \approx 10^6$. Counterstreaming instabilities due to relative motion of large groups of particles in the context of pulsar emission have been considered; they do not suffer from the problem of low beam densities, and the growth rates are usually limited by the necessarily high Lorentz factors [13]. In the existing literature [13,14], the existence of counterstreaming

that is adequate to account for the wave growth is postulated, for example, as a result of bursty pair generation. An advantage of the oscillating model is that the relative motion of the two components has a clear physical origin. This model can allow more efficient growth of a streaming instability through two effects: the absence of relativistic suppression of the growth rate at phases where the relative streaming is nonrelativistic or mildly relativistic, and the relatively slow net outflow allowing more time for wave growth. The model may also account for OPMs through mode coupling at phases where the oscillating counterstreaming has Lorentz factor close to $\gamma_{\max}$, and the cyclotron frequency is near its minimum, which can be below the frequency of the escaping radiation at its source.

In this paper we consider the dispersive properties of a magnetized, relativistic, counterstreaming, electron-positron plasma and their possible implications for instabilities and mode coupling in a pulsar magnetosphere. The application to pulsar emission involves wave propagation in an intrinsically time-dependent medium. This allows the possibility of instability at one phase of the oscillation and mode coupling at another phase. Rather than the wave growth and mode coupling regions being separated in space, as in a conventional model, they are separated in time (phase of the oscillation) in an oscillating model. Although there is an extensive literature on mode coupling in a spatially inhomogeneous, stationary plasma, we are unaware of any discussion of mode coupling in a temporally varying, homogeneous medium. We comment briefly on the implication, basing our comments on Hamilton's equations for a ray in a medium in which the temporal variations depend on a single parameter (the counterstreaming speed).

Our basic model is a counterstreaming electron-positron pair plasma, such that electrons move in one direction and positrons in the other along magnetic field lines, with speed βc and Lorentz factor $\gamma=(1-\beta^2)^{-1/2}$, oscillating between $\gamma=1$ and $\gamma=\gamma_{\max}\sim 10^6$. Although the medium is time dependent, we assume that it is locally stationary in treating the wave dispersion. This is a valid approximation provided that the wave frequency ω is much greater than the oscillation frequency; for typical model parameters the ratio is $\gtrsim 10^3$ [11]. The oscillating model implies an electric field parallel to the magnetic field, and we neglect the direct effect of the electric field on the plasma dispersion. The effect of a parallel electric field in wave dispersion in the birefringent vacuum is known, but we are unaware of any discussion on its effect on plasma dispersion. The vacuum contribution may be treated using the Heisenberg-Euler Lagrangian [15], and it is negligible here. For simplicity we assume that the number densities of electrons and positrons are equal.

In Sec. II we summarize the properties of the wave modes in the absence of streaming; these properties are helpful in understanding the mode structure in the presence of counterstreaming. In Sec. III we discuss the case of parallel propagation (i.e., $\mathbf{k}\|\mathbf{B}$), and we extend the discussion to slightly oblique angles in Sec. IV. Mode coupling in a time-dependent, homogeneous medium is discussed in Sec. V. The application to pulsars is discussed in Sec. VI, and the conclusions are summarized in Sec. VII.

II. NONSTREAMING, COLD, PURE-PAIR PLASMA

Before considering the effect of counterstreaming, it is relevant to review wave dispersion in a cold, magnetized pair plasma in the absence of streaming, $\beta=0$. The inclusion of positrons introduces additional modes that have no counterpart in the familiar case of a cold electron gas, often called the "magnetoionic" theory [16]. The counterpart of the magnetoionic theory for equal numbers of electrons and positrons ("pure pair plasma") [17,18] is the relevant case here. A pure pair plasma is nongyrotropic: the contributions of each species of particle to the off-diagonal terms in the dielectric tensor are proportional to the sign of the charge, and the terms cancel exactly for nonstreaming electrons and positrons. Such a dielectric tensor is equivalent to that for a uniaxial crystal with dielectric constants $K_\perp=1-\omega_p^2/(\omega^2-\Omega_e^2)$ and $K_\parallel=1-\omega_p^2/\omega^2$, implying dispersion relations $n^2=K_\perp$ for the ordinary mode and $n^2=K_\perp K_\parallel/K_L$, with $K_L=K_\perp \sin^2\theta+K_\parallel\cos^2\theta$, for the extraordinary mode. Unfortunately the conventional use of "ordinary" and "extraordinary" in magnetoionic theory is based on a different criterion [16], and is inconsistent with the usage, that we adopt here, for a uniaxial crystal. In this paper, Ω_e is the cyclotron frequency, θ is the angle between the direction of wave propagation and the magnetic field, ω_p is the plasma frequency, defined by $\omega_p^2=e^2n_0/\epsilon_0 m$, where n_0 is the sum of the number densities of electrons and positrons, and $n=kc/\omega$ is the refractive index.

When viewed as equations for ω^2 as a function of $k^2=n^2\omega^2/c^2$, the dispersion relation $n^2=K_\perp$ becomes a quadratic equation, and the dispersion relation $n^2=K_\perp K_\parallel/K_L$ becomes a cubic equation. The dispersion relations for the two ordinary modes are $\omega^2=\omega_{o\pm}^2$, with

$$\omega_{o\pm}^2=\frac{1}{2}(\omega_p^2+\Omega_e^2+k^2c^2) \pm \frac{1}{2}[(\omega_p^2+\Omega_e^2+k^2c^2)^2-4\Omega_e^2k^2c^2]^{1/2}. \quad (1)$$

The higher-frequency branch has a cutoff $k^2\to 0$ at $\omega^2=\omega_p^2+\Omega_e^2$ and approaches the light line $\omega^2=k^2c^2$ at high frequencies. The lower-frequency branch extends from $\omega=0$ at $k=0$ to a resonance $k\to\infty$ at the cyclotron frequency. The ordinary mode is strictly transverse and has no dependence on angle θ so that its properties are the same for oblique as for parallel propagation.

The dispersion relation for the extraordinary modes is

$$(\omega^2-\omega_p^2)(\omega^2-\omega_{o+}^2)(\omega^2-\omega_{o-}^2)+k^2c^2\omega_p^2\Omega_e^2\sin^2\theta=0. \quad (2)$$

The solutions simplify for parallel propagation, when the final term in Eq. (2) is absent. Then Eq. (2) factorizes into $\omega^2=\omega_p^2$, which corresponds to a longitudinal mode, and a quadratic equation, which corresponds to two transverse modes that are degenerate with the two ordinary modes (and that are polarized orthogonally to the ordinary modes). The dispersion curves appear in Fig. 1. The dispersion line $\omega^2=\omega_p^2$ crosses the lower-frequency branch of the degenerate ordinary and extraordinary modes at $k^2c^2=\omega_p^2\Omega_e^2/(\Omega_e^2-\omega_p^2)$.

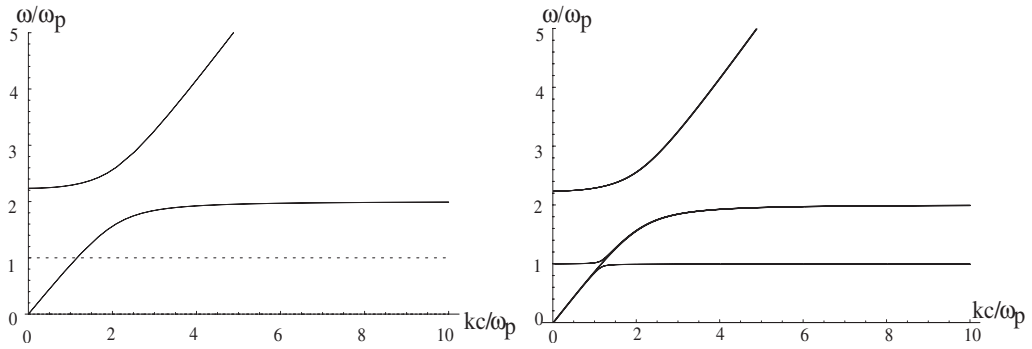

FIG. 1. Dispersion curves ω vs k in normalized units for (left) parallel propagation and (right) slightly oblique propagation in a cold pure pair plasma with $\Omega_e=2\omega_p$. Dashed lines in the left panel are longitudinal parts and solid lines are transverse parts. In the right panel $\theta=0.1$ rad to show the separation of the o and x modes.

For slightly oblique propagation the longitudinal mode and the lower-frequency branch of the extraordinary mode reconnect separating the extraordinary mode into three branches, one from $\omega=0$ to a resonance near $\omega=\omega_p$, the second from the cutoff at $\omega=\omega_p$ to a resonance near $\omega=\Omega_e$, and the third branch is close to the upper-frequency branch of the ordinary mode. The dispersion curves are illustrated in Fig. 1.

The wave properties for a pair plasma are modified if the number densities of electrons and positrons are not strictly equal. One of the three (equal and opposite) pairs of off-diagonal terms in the dielectric tensor is then nonzero. If the difference between the number densities is sufficiently small, the resulting gyrotropy may be regarded as leading to a coupling between the ordinary and the extraordinary modes. In the opposite limit, where the admixture of positrons is small, the qualitative effect of the admixture on the magnetoionic theory is to introduce a resonance at $\omega=\Omega_e$ and to add an extra branch into both magnetoionic modes [19]. Although our assumption that the number densities are strictly equal is overly restrictive in discussing the nonstreaming case, it is not so restrictive in the presence of counterstreaming. Even for equal number densities, the inclusion of counterstreaming causes the pair plasma to be gyrotropic, such that the modes are elliptically polarized in general.

III. PARALLEL PROPAGATION IN A COUNTERSTREAMING PLASMA

A counterstreaming plasma has two components propagating in opposite directions. Here we consider counterstreaming of electrons and positrons, in a frame in which they have equal velocities. The components of the response tensor for a cold counterstreaming pair plasma are written in the Appendix. The wave properties for parallel propagation are discussed in this section.

A. Longitudinal modes

It is convenient to introduce the parameters

$$\omega_0 = \gamma\omega, \quad \omega_\parallel = \gamma k_\parallel \beta c. \tag{3}$$

The dispersion equation for longitudinal ($\mathbf{E}\parallel\mathbf{k}$) waves is

$$(\omega_0^2 - \omega_\parallel^2)^2 - \omega_p^2(\omega_0^2 + \omega_\parallel^2) = 0, \tag{4}$$

which we regard as a quadratic equation for ω_0^2 as a function of $\omega_\parallel^2$. The two solutions are given by

$$\omega_0^2 = \frac{1}{2}\omega_p^2 + \omega_\parallel^2 \pm \frac{1}{2}\omega_p^2[1 + 8\omega_\parallel^2/\omega_p^2]^{1/2}. \tag{5}$$

The high-frequency branch of Eq. (5) has a cutoff ($k=0$ implying $\omega_\parallel=0$) at $\omega=\omega_p/\gamma$, with the frequency increasing with increasing k, given approximately by

$$\omega \approx \begin{cases} \omega_p/\gamma + 3k^2\beta^2c^2\gamma/2\omega_p & \text{for } 8\omega_\parallel^2 \ll \omega_p^2, \\ k\beta c + \omega_p/2^{1/2}\gamma & \text{for } 8\omega_\parallel^2 \gg \omega_p^2. \end{cases} \tag{6}$$

This branch may be interpreted as the counterpart of the Langmuir wave mode, as may be seen by taking the nonstreaming limit $\beta\to 0$, where it reduces to $\omega=\omega_p$.

The low-frequency branch of Eq. (5) is real for $\omega_\parallel^2 > \omega_p^2$, and imaginary for $\omega_\parallel^2 < \omega_p^2$, with $\omega_0=0$ for $\omega_\parallel^2=\omega_p^2$. On the lower branch, in place of Eq. (6), one has

$$\omega \approx \begin{cases} ik\beta c & \text{for } 8\omega_\parallel^2 \ll \omega_p^2, \\ k\beta c - \omega_p/2^{1/2}\gamma & \text{for } 8\omega_\parallel^2 \gg \omega_p^2. \end{cases} \tag{7}$$

In the absence of streaming $\beta\to 0$ the lower-frequency branch disappears.

B. Instability

The lower frequency branch includes a streaming instability: for $\omega_\parallel^2 < \omega_p^2$, ω_0^2 is negative, implying a mode with a purely imaginary frequency. The maximum (as a function of k) growth rate occurs when $\omega_\parallel^2=3\omega_p^2/8$, and has the value

$$\Gamma_{\max} = \left(\frac{1}{8}\right)^{1/2}\frac{\omega_p}{\gamma}, \quad k = \left(\frac{3}{8}\right)^{1/2}\frac{\omega_p}{\gamma\beta c}. \tag{8}$$

This maximum growth rate decreases as a function of the Lorentz factor of the streaming, so that the most favorable condition for growth is when the streaming is nonrelativistic or mildly relativistic, i.e., $\gamma\approx 1$.

C. Transverse dispersion equation

The dispersion equation for parallel-propagating transverse waves is

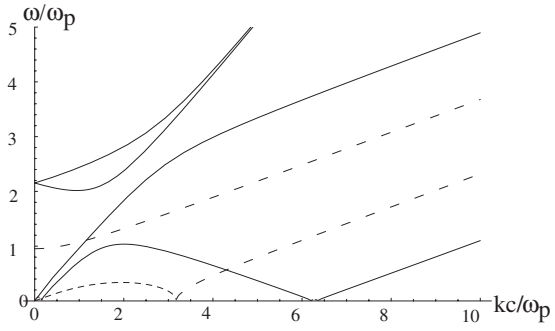

FIG. 2. Dispersion curves ω vs k in normalized units for parallel propagation in a cold counterstreaming plasma with $\beta=0.3$, $\Omega_e=2\omega_p$. Dotted lines show imaginary parts, dashed lines show longitudinal real parts and solid lines show transverse real parts.

$$\begin{vmatrix} 1-n^2+\Pi^{11} & \Pi^{12} \\ -\Pi^{12} & 1-n^2+\Pi^{11} \end{vmatrix} = 0, \tag{9}$$

where expressions for the terms Π^{11} and Π^{12} are written down in the appendix. Regarding Eq. (9) as a quadratic equation for $1-n^2$, where $n^2=k^2c^2/\omega^2=\omega_\parallel^2/\beta^2\omega_0^2$ is the square of the refractive index, its solutions are given by

$$1-n^2=\frac{\omega_p^2}{\omega^2}\frac{(\omega_0^2-\omega_\parallel^2)^2-\Omega^2(\omega_0^2+\omega_\parallel^2)}{(\omega_0^2+\omega_\parallel^2-\Omega^2)^2-4\omega_0^2\omega_\parallel^2} \pm \frac{\omega_p^2}{\omega^2}\frac{\Omega\omega_\parallel(\omega_0^2-\omega_\parallel^2+\Omega^2)}{(\omega_0^2+\omega_\parallel^2-\Omega^2)^2-4\omega_0^2\omega_\parallel^2}, \tag{10}$$

which may also be written

$$\frac{\omega^2-k^2c^2-\omega_p^2}{\omega^2}-\frac{\omega_p^2\Omega(\Omega+\omega_\parallel)(\omega_0\pm\omega_\parallel-\Omega)(\omega_0\mp\omega_\parallel+\Omega)}{\omega^2 D}=0, \tag{11}$$

where

$$D=(\omega_0+\omega_\parallel+\Omega)(\omega_0+\omega_\parallel-\Omega)(\omega_0-\omega_\parallel+\Omega)(\omega_0-\omega_\parallel-\Omega). \tag{12}$$

The solutions of Eq. (11) for ω_0^2 are

$$\omega_0^2=[\omega_0^2]_{\pm\sigma}=\frac{1}{2}[\gamma^2k^2c^2+(\omega_\parallel\pm\Omega)^2+\gamma^2\omega_p^2]+\frac{\sigma}{2}\Delta_\pm,$$

$$\Delta_\pm^2=[\gamma^2(k^2c^2+\omega_p^2)-(\omega_\parallel\pm\Omega)^2]^2+4\gamma^2\omega_p^2\Omega(\Omega\mp\omega_\parallel), \tag{13}$$

with $\sigma=\pm$.

The dispersion curves corresponding to the solutions (13) are plotted in Fig. 2. The four modes (13) may be regarded as split versions of the ordinary and extraordinary modes discussed in Sec. II. This may be seen by noting that the nonstreaming limit corresponds to $\omega_\parallel\to 0$, $\Delta_+\to\Delta_-$ in Eq. (13). The upper-frequency branches correspond to a streaming-induced splitting of the upper-frequency branch of the nonstreaming ordinary and extraordinary modes; these nonstreaming modes are degenerate for parallel propagation, and they remain degenerate for parallel propagation when streaming is included. For small k, the two lower-frequency branches may be approximated by

$$\omega_0^2\approx\begin{cases}\Omega^2+\gamma^2\omega_p^2-2\Omega\beta\left(\dfrac{\Omega^2}{\gamma^2\omega_p^2+\Omega^2}\right)k_\parallel c, \\ \dfrac{\beta\gamma^2\omega_p^2\Omega}{\gamma^2\omega_p^2+\Omega^2}kc.\end{cases} \tag{14}$$

These modes may also be regarded as split versions of the lower-frequency branch of the degenerate modes discussed in Sec. II.

D. Instability

An instability occurs in the lowest-frequency branch of the transverse modes in two ranges of k. The condition for instability, $\omega_0^2<0$, for the lower branch in Eq. (13) becomes

$$(\Omega-\omega_\parallel)(k^2c^2\Omega-k^2c^2\omega_\parallel-\omega_p^2\omega_\parallel)\le 0. \tag{15}$$

There is a region of instability between $k=0$ and $k=k_-$, a region of stability (i.e., the mode is real) between $k_-<k<k_+$, another region of instability in the range $k_+<k<\Omega/\beta c$, and the mode is real for $k>\Omega/\beta c$, with

$$k_\pm c=\frac{\Omega}{2\beta\gamma}\pm\frac{\Omega}{2\beta\gamma}\left(1-\frac{4\omega_p^2\beta^2\gamma^2}{\Omega^2}\right)^{1/2}. \tag{16}$$

The locations of these two solutions are shown in Fig. 3, k_- in the left panel, and k_+ in the right.

IV. PROPAGATION AT A SMALL ANGLE

Three new features appear for oblique propagation. First, the modes are no longer strictly longitudinal or transverse: all oblique modes have both longitudinal and transverse components. In particular, the region of k where growth occurs at zero frequency for parallel propagation in the lower-frequency longitudinal mode is modified for a small angle of propagation, with the real part of the frequency changing from zero to a small, nonzero value. The instability in the parallel-propagating transverse waves is not changed significantly at small angles of propagation. Second, as is well known, where longitudinal and transverse modes cross in the limit of parallel propagation, they reconnect for oblique propagation. The modes usually deviate away from each other, with the polarization changing rapidly from nearly longitudinal to nearly transverse, or vice versa. Third, in the presence of streaming an alternative type of reconnection is possible: two real modes that cross in the parallel limit can separate with a pair of complex modes connecting them. In this section we discuss the latter two of these features, starting with the alternative type of reconnection.

A. Intrinsically oblique instabilities

A new feature of oblique propagation is the appearance of a complex conjugate pair of solutions, where two real modes (corresponding to the lowest transverse and the lower longitudinal modes) merge to become a pair of modes with one growing and the other decaying. Figure 4 illustrates the wave

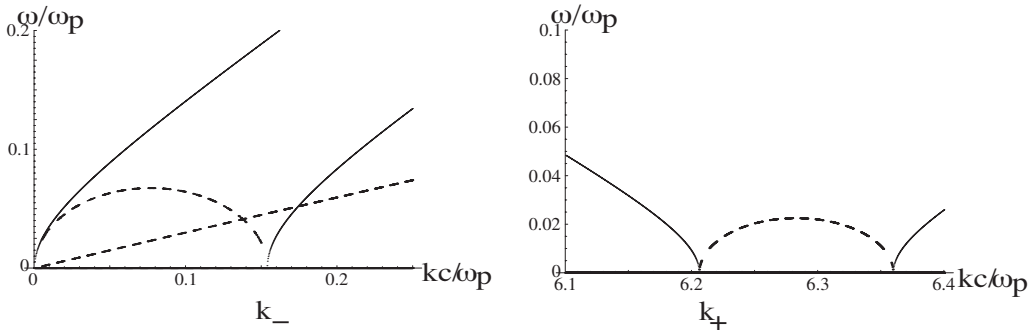

FIG. 3. Magnified dispersion curves ω vs k in normalized units for two regions of Fig. 2. The parameter values are $\Omega_e=2\omega_p$. Dashed lines show imaginary parts and solid lines show real parts. Left: a zoomed region showing the imaginary part of the lowest transverse mode near $k=0$. Right: a zoomed region showing the imaginary part of the lowest transverse mode near $k=k_+$ ($k_+c/\omega_p\approx 6.2$ for the chosen parameter values).

modes for oblique propagation. The complex modes appear near $kc/\omega_p\simeq 5.8$, which corresponds to the intersection of $\omega=\Omega/\gamma-\beta k$ and the lower branch of the longitudinal mode, $\omega=k\beta c-\omega_p/\sqrt{2}\gamma$, at $k=\frac{1}{2}\beta\gamma(\Omega+\omega_p/\sqrt{2})$. This region of wave growth is in addition to those identified for parallel propagation.

The various interactions between modes in the limit of parallel propagation are modified at small angles of propagation, as displayed in the various subfigures indicated by the labels in Fig. 5. In some cases the modification is a deviation in which the two modes reconnect into two different real modes, and in other cases two real modes become a complex conjugate pair of modes, of which one is necessarily a growing mode. The interactions at different points are displayed as close-ups in Fig. 5, with the labels indicating the corresponding points on the main diagram.

Consider the specific dispersion curve, for ω as a function of k, in Fig. 5 that corresponds to the lowest transverse branch for parallel propagation. This branch begins at $\omega=0$ for $k=0$, and is initially imaginary, becoming real and propagating at $kc/\omega_p\simeq 0.1$. As the intersection labeled 2 is approached, it deflects away from the other modes and remains a single real mode, and again at intersection 3. At intersection 4, it joins another mode and forms a pair of complex

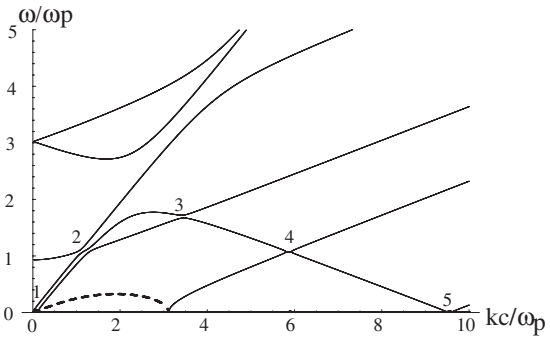

FIG. 4. Dispersion curves ω vs k in normalized units for nearly parallel propagation ($\theta=0.1$ rad) in a cold counterstreaming plasma with $\beta=0.3$, where $\Omega_e=3\omega_p$. Dashed lines are imaginary parts and solid lines are real parts. Numbers indicate regions expanded in Fig. 5.

conjugate solutions, which then become real again for higher k. The physical implication of intersection 4 for propagation through a slowly varying medium is not clear.

The foregoing results are for $\Omega_e=2\omega_p$, which is not realistic for a pulsar, which has $\Omega_e\gg\omega_p$. For much larger values of Ω_e/ω_p, the topological structures of the dispersion curves are similar to those for $\Omega_e/\omega_p\approx 1$. Figure 6 illustrates the case $\Omega_e/\omega_p\approx 1000$ and $\gamma\approx 22$. For the parameters in Fig. 6, the curves appear as straight lines, which lines are apparent in the upper right of Fig. 4. The coupling points are concentrated in a region near the origin, in a region at around $kc/\omega_p\approx 2-\omega/\omega_p\approx 2$, and in a region around $kc/\omega_p\approx 4-\omega/\omega_p\approx 0$. The region near the origin contains the cutoff for the almost longitudinal mode, and the structure shown in panel 1 of Fig. 5. The structure in panels 2, 3, and 4 of Fig. 5 are in the region around $(\omega/\omega_p, kc/\omega_p)\approx(20,20)$ in Fig. 6, and panel 5 of Fig. 5 corresponds to the feature at $(\omega/\omega_p, kc/\omega_p)\approx(40,0)$ in Fig. 6. Note that the apparent line along $\omega=kc$ in Fig. 6 is actually multiple lines very close together.

B. High-velocity counterstreaming

At high relative streaming factor $\beta\approx 1$, $\gamma\gg 1$, both the plasma frequency and cyclotron frequency are reduced, by factors $1/\gamma^{1/2}$ and $1/\gamma$, respectively. The mode structure changes in two ways at high γ. First, all of the mode interaction structure is compressed into a small region of ω-k space near the origin. Outside this region all modes are vacuumlike: the dispersion curves approach a set of lines parallel to the light lines $\omega=kc+C$, where C is a constant that depends on the mode. Second, the two regions of instability in the lowest transverse branch become a single region near $\beta^2\gamma=\Omega^2/4\omega_p^2$; this occurs as the two points k_- and k_+ in Eq. (16) coalesce.

A graph for the case $\gamma\simeq 22$ ($\beta=0.999$) is shown in Fig. 7. Note that the two highest modes are off the top of the vertical axis, and that the lowest frequency mode corresponds to the longitudinal mode. There are two major differences from the low velocity case. First, where the higher almost-longitudinal mode and the almost-transverse modes interact, the lowest almost-transverse mode is imaginary, and so is not coupled

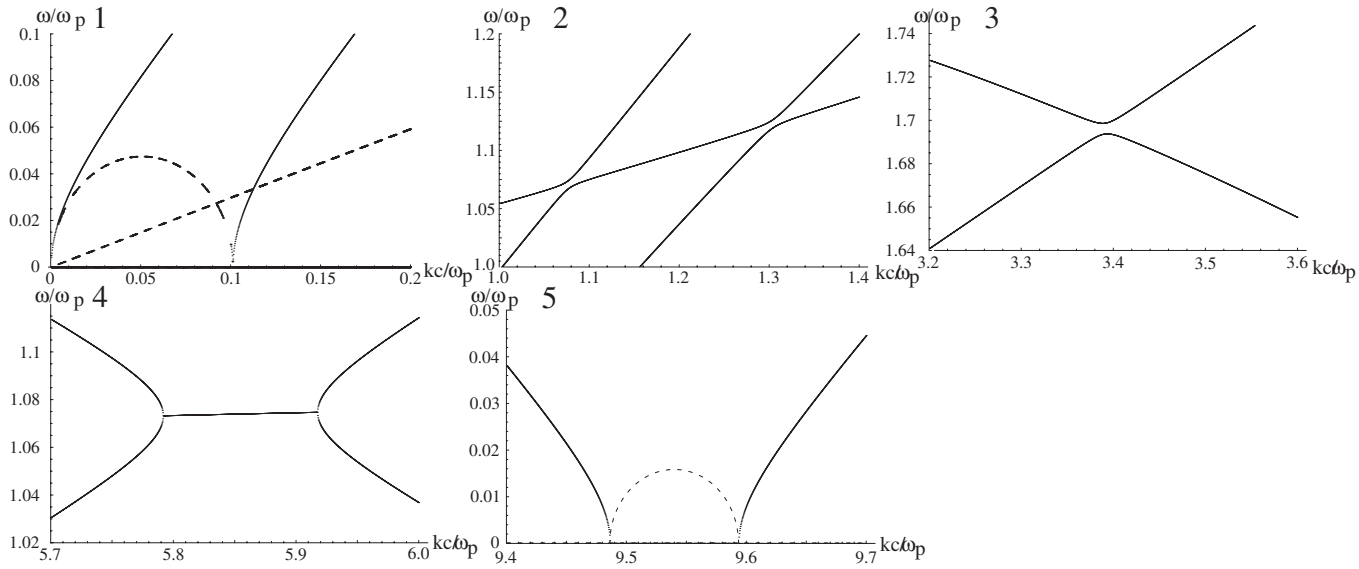

FIG. 5. Dispersion curves ω vs k in normalized units for propagation at a small angle (θ=0.1 rad) in a cold counterstreaming plasma with β=0.3, where $\Omega_e=3\omega_p$. These subfigures show close-up views of the numbered regions in Fig. 4, and display the behavior in the interaction regions.

to the other modes. The second significant change is the absence of the coupling at intersection 4 in Fig. 4, which is due to the transverse branch not being a real mode where it would intersect the longitudinal branch.

V. SLOWLY VARYING MEDIUM

In an oscillating model of a pulsar magnetosphere [11,12], the medium is time dependent. Provided the temporal changes, and any spatial changes, are sufficiently gradual, the propagation of a wave through the medium can be treated using geometric optics, modified by inclusion of mode coupling. Let $\omega=\omega_M(\mathbf{k})$ be the dispersion equation for a wave mode M in a locally homogeneous, stationary medium. The inclusion of slow variations of the medium in space and time leads to the local dispersion relation being a function of space and time: $\omega=\omega_M(\mathbf{k};\mathbf{x},t)$. The propagation of rays may then be treated using a Hamiltonian formalism, with $\omega_M(\mathbf{k};\mathbf{x},t)$ playing the role of the Hamiltonian.

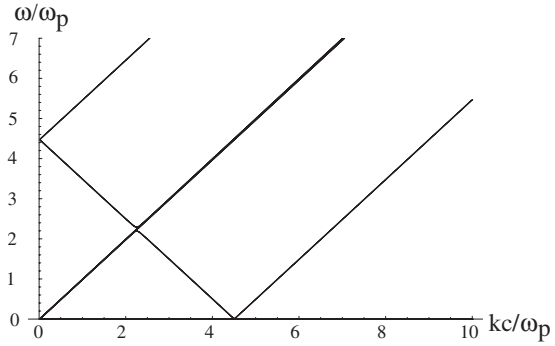

FIG. 6. Dispersion curves ω vs k in normalized units for nearly parallel propagation (θ=0.1 rad) in a cold counterstreaming plasma with $\gamma\simeq 22.4$ and $\Omega=1000\omega_p$.

A. Hamilton's equations

In the geometric optics approximation, the propagation of a ray is determined by Hamilton's equations

$$\dot{\mathbf{x}}=\frac{\partial\omega_M}{\partial\mathbf{k}},\quad \dot{\mathbf{k}}=\frac{\partial\omega_M}{\partial\mathbf{x}},\quad \dot{\omega}=\frac{\partial\omega_M}{\partial t}, \tag{17}$$

where the overdot denotes differentiation with respect to an affine parameter that may be interpreted as time along the ray path, and where the arguments $\mathbf{k}$, $\mathbf{x}$, t of ω_M are implicit. Here we are concerned primarily with the effect of temporal variations. For simplicity we consider a homogeneous medium, and we further assume that the temporal variations are due only to the changing relative streaming velocity, described by the Lorentz factor $\gamma(t)$. The last of the Eqs. (17) then gives

$$\dot{\omega}=\frac{d\gamma}{dt}\frac{\partial\omega_M}{\partial\gamma}. \tag{18}$$

The assumption that ω_M depends on t on through its dependence on $\gamma(t)$ allows one to integrate Eq. (18) to find that the

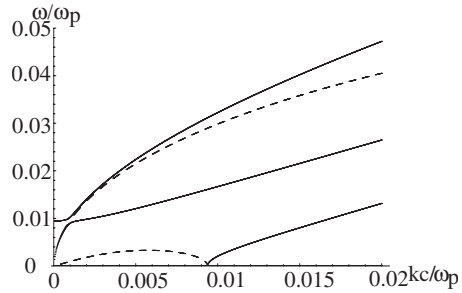

FIG. 7. Dispersion curves ω vs k in normalized units for nearly parallel propagation (θ=0.1 rad) in a cold counterstreaming plasma with β=0.999, where $\Omega_e=3\omega_p$. Dashed lines show imaginary parts and solid lines show real parts.

wave frequency varies with time such that the instantaneous dispersion relation is always satisfied. We write this condition as $\omega(t)=\omega_M(\mathbf{k};t)$.

B. Mode coupling

The spatial and temporal variations imply a coupling between modes: radiation initially in one mode becomes a mixture of two or more modes. Coupled equations for the modes can be derived provided that there are two distinct time and space scales: on a fast and small scale one Fourier transforms and identifies the waves modes, and variations on a slow and large scale lead to coupling between these modes. Mode coupling in a slowly varying medium is weak except near coupling points, where the dispersion curves intersect. The coupling points of relevance here are defined by the intersections of the various dispersion curves in the limit of parallel propagation. There are two limiting cases of coupling at any coupling point. If the coupling is weak, a wave approaching a coupling point stays in the actual mode (for oblique propagation) as the dispersion curve deviates away from the coupling point, with only a small leakage from the initial mode to the other mode. There is a rapid change in the polarization near the coupling point, and in weak coupling the polarization of the wave follows this change. If the coupling is strong, a wave approaching a coupling point propagates through it as it would in the strictly parallel case, jumping from one actual mode to the other, with only a small fraction of the incident energy remaining in the initial mode. The polarization of the wave effectively ignores the rapid change in the modes, and preserves its initial value. Coupling is strong if the angle of propagation is sufficiently small as the coupling point is approached, and for larger angles the coupling is weak. This angle, which depends on the details of the problem, defines a "window:" this phenomenon was first discussed in the context of ionospheric sounding, where coupling of the o mode to the z mode is effective within the "Ellis window" [20]. In the temporally varying medium, a coupling point is approached as a function of time, and the effectiveness of the coupling is sensitive to the rate of change of the wave frequency with time, which effectively determines the size of the "window." Although these points are obvious from a qualitative viewpoint, at present there is no quantitative theory for mode coupling in a time-varying medium.

In the simple case discussed above, where the time dependence is in only the streaming velocity and the medium is homogeneous, the wave frequency follows the dispersion curve, and so its variation with time can be inferred from its variation with β or γ. The frequency is shown as a function of β for a given wave number, in Fig. 8 (the specific case shown is $kc/\omega_p=2.5$).

It is apparent from Fig. 8 that ω can either decrease or increase as a function of β, and that there are only four regions where coupling can be effective: two near zero real frequency, and two at nonzero frequency. For example, consider waves generated in the growth region at zero real frequency and small k. As β increases, ω changes from imaginary to real, and then increases until it approaches the coupling point just below $\beta=0.6$. The wave passes through a range of β where ω is complex, and after passing through this region, there are two possibilities: the frequency increases following the upper curve or decreases following the lower curve. We suspect that there is a counterpart of strong coupling, such that the wave follows the upper curve, and a counterpart of weak coupling such that it follows the lower curve. An important effect of this expected coupling is that it allows the conversion of the high-growth electrostatic waves into electromagnetic waves, which may then be converted into OPMs as discussed below. Thus we expect that through this time-dependent mode coupling the electrostatic waves can be largely responsible for driving electromagnetic emission. In the absence of a theory for mode coupling under these conditions, we are unable to discuss this point further.

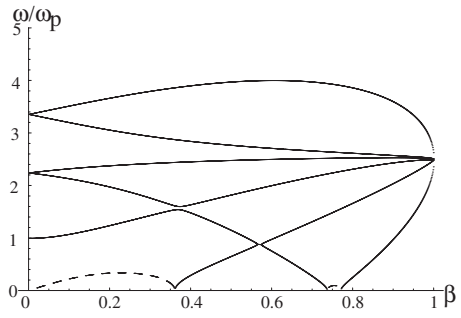

FIG. 8. Dispersion curves ω vs β in normalized units for nearly parallel propagation ($\theta=0.1$ rad) in a cold counterstreaming plasma with $kc/\omega_p=2.5$, where $\Omega_e=3\omega_p$. Dashed lines show imaginary parts and solid lines show real parts.

VI. APPLICATION TO PULSAR MODEL

In the oscillating model for the pulsar magnetosphere discussed in Refs. [11,12], dispersion in the counterstreaming pair plasma plausibly satisfies most of the properties assumed in the foregoing discussion. A proviso is that the assumption that the electrons and positrons are cold in their respective rest frames is not expected to be the case, with at least a mildly relativistic spread expected [6]. This probably invalidates our results in the limit of nonrelativistic streaming, where the streaming speed is smaller than the intrinsic spread in the speeds of the electrons and positrons. Additionally, in this region the acceleration of the particles is at its maximum value, and a strong electric field is present. As we are not aware of a theory for the response of an intrinsically time-dependent medium, we treat the plasma as stationary at any point for the purposes of calculating the wave dispersion. This neglects the effect of the acceleration on the growth rate, and of the electric field on the wave dispersion.

The inclusion of an electric field has not been discussed in the literature to our knowledge. The plasma becomes intrinsically time dependent due to the constant acceleration provided by the field. We work in the Fourier domain which is meaningful provided that the frequencies involved are large compared with the frequency of the oscillating electric field. With these provisos, our model should provide a reasonable guide to the expected properties of the wave dispersion.

A. Wave growth over many oscillations

The key feature of the oscillating model of pulsar magnetospheres is the intrinsic time dependence of the medium. In a conventional model, the bulk outflow speed exceeds the relative streaming speed, and wave growth is limited by the outflow and the variation with height. As a growing wave (at a fixed frequency) propagates outward, the frequency range for wave growth moves to lower frequencies, as the natural frequencies of the plasma decrease with height along the ray path, and growth stops when the wave frequency moves out of the frequency range where growth occurs. Effective growth requires a large growth rate over a broad frequency range in a region where the plasma frequency does not change rapidly with distance along the ray path. In the oscillating model, the ratio of the outward flow speed to the relative streaming is reversed, and growth in one (half) phase of the oscillation is limited by temporal changes in the medium. Growth is strongest during phases where the relative streaming velocity is small (but not smaller than the intrinsic spread in the speeds of the electrons and positrons). A wave may experience many bursts of growth (two per oscillation period) before escaping. These two effects, larger growth for mildly relativistic streaming, and growth over many phases of the oscillation, can potentially enhance the net growth to a much greater value than in a nonoscillating model.

Specifically, consider parallel longitudinal waves generated in the phase of the oscillation where the relative streaming is nonrelativistic $[\gamma(t) \approx 1]$. These waves have $\omega=0$, and grow around a preferred k during the nonrelativistic phase. As $\gamma(t)$ increases the waves change from intrinsically growing to propagating waves, as discussed in connection with Fig. 8. Provided these waves remain in a mode of the time-varying medium, their original properties are restored when $\gamma(t)$ returns to its initial nonrelativistic value. In practice the pulsar magnetosphere is far from homogeneous and the conditions under which this idealized, periodic evolution might occur require detailed investigation, which we do not attempt here.

B. Mode coupling

The oscillating model provides a possible explanation for the enigmatic OPMs. In many cases OPMs seem to require a roughly equal mixture of two elliptically polarized modes, which is strongly indicative of mode coupling associated with a cyclotron resonance. Assuming that the waves are initially generated as electrostatic waves, our model allows them to encounter a cyclotron resonance near their source. By way of illustration consider a surface magnetic field of 10^8 T and $\gamma_{\max}=10^6$; then the minimum cyclotron frequency is comparable with the frequency of the observed radiation for a source at ten stellar radii, and for the favored source heights of several tens of stellar radii, the cyclotron resonance is encountered in the source region four times per oscillation period. As the frequency passes through the cyclotron resonance, each mode changes from nearly linear, through circular to nearly linear in the orthogonal sense [21]. A wave remains in its initial mode and follows this change only if the two modes get out of phase faster than the rate of change of the shape of the polarization ellipse. For example, for a source region at 100 stellar radii and a wave frequency 10^3 times the oscillation frequency, the Lorentz factor passes through a phase with $\gamma \approx 10^3$ in a time Δt of order 10^{-3} of an oscillation period, implying $\omega \Delta t \approx 1$, which is the threshold for strong mode coupling. A single initial mode is converted into a roughly equal mixture of two modes for $\omega \Delta t \approx 1$. These numbers allow effective mode coupling.

VII. CONCLUSIONS AND DISCUSSION

We derive the response for a cold, counterstreaming pair plasma in general and give expressions for the specific case of equal number densities. For parallel propagation, the dispersion equation factorizes into equations for two longitudinal and four transverse modes. Instabilities occur in both the lowest longitudinal and lowest transverse modes. The dispersion curves for longitudinal and transverse modes intersect at several points, and for propagation at small oblique angles, the modes reconnect either by deflecting away from each other, or by two real modes joining to become a complex conjugate pair. For illustrative purposes, we plot these dispersion relations for cases where the relative streaming is nonrelativistic and the cyclotron frequency is twice or three times the plasma frequency.

The motivation for this investigation is the application to the oscillating model of pulsar magnetospheres. The model introduces several possibly important effects that are absent in conventional discussions of pulsar radio emission mechanisms: wave frequencies changing periodically with time (in phase with the oscillations), wave growth in bursts over many oscillation periods, and mode coupling associated with the cyclotron resonance in the source region. The model offers the possibility of overcoming the slowness of wave growth in conventional models: the growth rate is largest during the phase where the counterstreaming is mildly relativistic, and this occurs twice per period of the oscillation and can continue over many oscillations. Another feature is that near the phase of the oscillations where the Lorentz factor is near its maximum $\gamma_{\max} \sim 10^6$ the cyclotron resonance crosses (as a function of phase) the wave frequency in the source region. Mode coupling associated with such a crossing provides a possible explanation for the almost ubiquitous phenomenon of orthogonally polarized modes. To analyze this effect in detail we need a theory that is not yet available: mode coupling due to intrinsically time-dependent effects in the medium. Without a detailed theory for such mode coupling we are unable to give a quantitative discussion of how longitudinal waves become transverse waves. One feature that we note is that Hamilton's equations imply that the wave frequency, for waves in an arbitrary mode M, evolves following the instantaneous dispersion relation $\omega=\omega_M(\mathbf{k},t)$ for the given mode as the counterstreaming speed β changes. This enables one to determine how the frequency varies with β (at fixed k in a homogeneous model), except where two dispersion curves cross at a coupling point. Mode coupling is important near coupling points, and the theory needed is that for mode coupling due to temporal changes at a coupling point.

The assumption that the electrons and positrons are cold in their respective rest frames is justifiable, as a first approximation, provided that the streaming speed is much greater than the intrinsic spread in velocities in the rest frames. We have in hand the formal generalization to the case where the electrons and positrons have one-dimensional relativistic thermal distributions in their rest frames. However, even for parallel propagation, the transcendental functions in the dispersion equation preclude finding general analytic solutions, and the richness of the detailed results is overwhelming. The cold plasma case considered in the present paper is an essential preliminary to detailed consideration of this more general case. A next step is to consider how thermal effects modify the wave properties derived here.

APPENDIX: COLD COUNTERSTREAMING PAIR PLASMA

There are two cases of interest here, the case of two counterstreaming electron plasmas and the case of counterstreaming electron and positron plasmas. Only the gyrotropic terms Π^{12}, Π^{21}, Π^{23}, and Π^{32} differ in the two cases.

The nongyrotropic space components of $\Pi^{\mu\nu}(k)$ for cold, magnetized, counterstreaming electrons and positrons or electrons and electrons with number densities $n^{\pm}=\frac{1}{2}n(1\pm\Delta)$, $\Delta=(n^+-n^-)/(n^++n^-)$, $n=n^++n^-$ (defined in the respective rest frame of each component) may be written

$$\Pi^{\mu\nu}(k)=\bar{\Pi}^{\mu\nu}(k)+\Delta\hat{\Pi}^{\mu\nu}(k), \tag{A1}$$

where the space components of $\Pi^{\mu\nu}(k)$ are

$$\bar{\Pi}^{11}=\bar{\Pi}^{22}=-\frac{e^2n}{m}\frac{(\omega_0^2-\omega_\parallel^2)^2-\Omega^2(\omega_0^2+\omega_\parallel^2)}{(\omega_0^2+\omega_\parallel^2-\Omega^2)^2-4\omega_0^2\omega_\parallel^2},$$

$$\bar{\Pi}^{33}=-\frac{e^2n}{m}\left[\frac{\omega^2(\omega_0^2+\omega_\parallel^2)}{(\omega_0^2-\omega_\parallel^2)^2}+\frac{\omega_\perp^2(\omega_0^2+\omega_\parallel^2-\Omega^2)}{(\omega_0^2+\omega_\parallel^2-\Omega^2)^2-4\omega_0^2\omega_\parallel^2}\right],$$

$$\bar{\Pi}^{13}=\bar{\Pi}^{31}=-\frac{e^2n}{m}\frac{\omega_\parallel\omega_\perp(\omega_0^2-\omega_\parallel^2+\Omega^2)}{(\omega_0^2+\omega_\parallel^2-\Omega^2)^2-4\omega_0^2\omega_\parallel^2},$$

$$\hat{\Pi}^{11}=\hat{\Pi}^{22}=-\frac{e^2n}{m}\frac{2\omega_0\omega_\parallel\Omega^2}{(\omega_0^2+\omega_\parallel^2-\Omega^2)^2-4\omega_0^2\omega_\parallel^2},$$

$$\hat{\Pi}^{33}=-\frac{e^2n}{m}\left[-\frac{2\omega^2\omega_0\omega_\parallel}{(\omega_0^2-\omega_\parallel^2)^2}-\frac{2\omega_\perp^2\omega_0\omega_\parallel^2}{(\omega_0^2+\omega_\parallel^2-\Omega^2)^2-4\omega_0^2\omega_\parallel^2}\right],$$

$$\hat{\Pi}^{13}=\hat{\Pi}^{31}=-\frac{e^2n}{m}\frac{\omega_0\omega_\perp(\omega_0^2-\omega_\parallel^2-\Omega^2)}{(\omega_0^2+\omega_\parallel^2-\Omega^2)^2-4\omega_0^2\omega_\parallel^2}. \tag{A2}$$

For counterstreaming electrons and positrons,

$$\bar{\Pi}^{12}=-\bar{\Pi}^{21}=i\frac{e^2n}{m}\frac{\Omega\omega_\parallel(\omega_0^2-\omega_\parallel^2+\Omega^2)}{(\omega_0^2+\omega_\parallel^2-\Omega^2)^2-4\omega_0^2\omega_\parallel^2},$$

$$\bar{\Pi}^{23}=-\bar{\Pi}^{32}=-i\frac{e^2n}{m}\frac{\Omega\omega_\perp(\omega_0^2+\omega_\parallel^2-\Omega^2)}{(\omega_0^2+\omega_\parallel^2-\Omega^2)^2-4\omega_0^2\omega_\parallel^2}, \tag{A3}$$

$$\hat{\Pi}^{12}=-\hat{\Pi}^{21}=i\frac{e^2n}{m}\frac{\Omega\omega_0(\omega_0^2-\omega_\parallel^2-\Omega^2)}{(\omega_0^2+\omega_\parallel^2-\Omega^2)^2-4\omega_0^2\omega_\parallel^2},$$

$$\hat{\Pi}^{23}=-\hat{\Pi}^{32}=-i\frac{e^2n}{m}\frac{2\Omega\omega_0\omega_\perp\omega_\parallel}{(\omega_0^2+\omega_\parallel^2-\Omega^2)^2-4\omega_0^2\omega_\parallel^2}, \tag{A4}$$

and for two counterstreaming electron plasmas

$$\bar{\Pi}^{12}=-\bar{\Pi}^{21}=i\frac{e^2n}{m}\frac{\Omega\omega_0(\omega_0^2-\omega_\parallel^2-\Omega^2)}{(\omega_0^2+\omega_\parallel^2-\Omega^2)^2-4\omega_0^2\omega_\parallel^2},$$

$$\bar{\Pi}^{23}=-\bar{\Pi}^{32}=-i\frac{e^2n}{m}\frac{2\Omega\omega_0\omega_\perp\omega_\parallel}{(\omega_0^2+\omega_\parallel^2-\Omega^2)^2-4\omega_0^2\omega_\parallel^2}, \tag{A5}$$

$$\hat{\Pi}^{12}=-\hat{\Pi}^{21}=i\frac{e^2n}{m}\frac{\Omega\omega_\parallel(\omega_0^2-\omega_\parallel^2+\Omega^2)}{(\omega_0^2+\omega_\parallel^2-\Omega^2)^2-4\omega_0^2\omega_\parallel^2},$$

$$\hat{\Pi}^{23}=-\hat{\Pi}^{32}=-i\frac{e^2n}{m}\frac{\Omega\omega_\perp(\omega_0^2+\omega_\parallel^2-\Omega^2)}{(\omega_0^2+\omega_\parallel^2-\Omega^2)^2-4\omega_0^2\omega_\parallel^2}, \tag{A6}$$

with $\omega_0=\gamma\omega$, $\omega_\perp=\gamma k_\perp\beta$, $\omega_\parallel=\gamma k_\parallel\beta$.

[1] D. B. Melrose, in *Proceedings of IAU 177, Astronomical Society of the Pacific Conference Series*, edited by M. Kramer, N. Wex, and R. Wielebinski (Astronomical Society of the Pacific, San Francisco, 2000), Vol. 202, pp. 721–726.

[2] M. M. McKinnon and D. R. Stinebring, Astrophys. J. **529**, 435 (2000).

[3] D. R. Stinebring, J. M. Cordes, J. M. Rankin, J. M. Weisberg, and V. Boriakoff, Astrophys. J. Suppl. Ser. **55**, 247 (1984).

[4] M. Gedalin, D. B. Melrose, and E. Gruman, Phys. Rev. Lett. **88**, 121101 (2002).

[5] J. A. Hibschman and J. Arons, Astrophys. J. **560**, 871 (2001).

[6] P. N. Arendt, Jr. and J. A. Eilek, Astrophys. J. **581**, 451 (2002).

[7] A. K. Harding and A. G. Muslimov, Astrophys. J. **508**, 328 (1998).

[8] A. Karastergiou, M. Kramer, S. Johnston, A. G. Lyne, N. D. R. Bhat, and Y. Gupta, Astron. Astrophys. **391**, 247 (2002).

[9] D. B. Melrose and Q. Luo, Mon. Not. R. Astron. Soc. **352**, 915 (2004).

[10] P. A. Sturrock, Astrophys. J. **164**, 529 (1971).

[11] A. Levinson, D. B. Melrose, A. Judge, and Q. Luo, Astrophys. J. **631**, 456 (2005).

[12] Q. Luo and D. B. Melrose, Mon. Not. R. Astron. Soc. (to be published).

[13] V. V. Usov, Astrophys. J. **320**, 333 (1987).

[14] V. N. Ursov and V. V. Usov, Astrophys. Space Sci. **140**, 325 (1988).

[15] D. B. Melrose, *Quantum Plasmadynamics*, Lecture Notes on Physics, No. 735 (Springer, Berlin, 2008).
[16] T. H. Stix, *The Theory of Plasma Waves* (McGraw-Hill, New York, 1962).
[17] G. P. Zank and R. G. Greaves, Phys. Rev. E **51**, 6079 (1995).
[18] G. A. Stewart and E. W. Liang, J. Plasma Phys. **47**, 295 (1992).
[19] D. B. Melrose, Plasma Phys. Contr. Fusion **39**, A93 (1997).
[20] K. G. Budden, *Radio Waves in the Ionosphere* (Cambridge University Press, Cambridge, 1961).
[21] D. B. Melrose and Q. Luo, Phys. Rev. E **70**, 016404 (2004).